1/22

CONCEPTS OF SATURATED ZONE MODELING FOR DEVELOPMENT OF A SITE-SCALE GROUNDWATER FLOW MODEL FOR YUCCA MOUNTAIN

Prepared for

U.S. Nuclear Regulatory Commission
Contract NRC–02–97–009

Prepared by

James R. Winterle
Melissa E. Hill
Chandrika Manepally

Center for Nuclear Waste Regulatory Analyses
San Antonio, Texas

February 2002

ABSTRACT

This report documents development of a three-dimensional, site-scale groundwater flow model for the saturated zone beneath Yucca Mountain, Nevada. The 30-layer model grid covers a 28 × 41-km [17.4 × 25.5-mi] area surrounding Yucca Mountain and explicitly includes 6 hydrostratigraphic layers and 13 structural features. The model was developed for use with the MODFLOW code using the Groundwater Modeling System, Version 3.1, user interface. Model calibrations to observed hydraulic heads were conducted by varying hydraulic conductivity values assigned to the model layers and structural features. Results indicate that a reasonable model calibration requires consideration of geologic structure and some type of barrier to lateral flow in the northern portion of the model. The northern barrier to flow is possibly explained by the presence of a caldera complex. Future uses of the model will include inverse optimization to obtain calibrations for various analyses to quantify the effects of data and model uncertainty on saturated zone flow paths. Such analyses are necessary to support development of the U.S. Nuclear Regulatory Commission (NRC) performance assessment code and to develop a knowledge base for risk-informed NRC review of the U.S. Department of Energy performance assessments for Yucca Mountain.

3/22

CONTENTS

Section			Page
ABSTRACT			iii
FIGURES			vii
TABLES			ix
ACKNOWLEDGMENTS			xi
1	INTRODUCTION		1-1
2	MODEL DESCRIPTION AND APPROACH		2-1
	2.1	Model Assumptions and Limitations	2-1
	2.2	Hydrogeologic Framework	2-1
	2.3	Model Domain and Grid	2-1
	2.4	Incorporation of Layer and Structural Features in the Model Grid	2-5
	2.5	Hydrologic Properties	2-8
		2.5.1 Hydrostratigraphic Layers	2-9
		2.5.2 Faults	2-11
		2.5.3 Caldera Complex	2-12
	2.6	Boundary Conditions	2-13
	2.7	Model Calibration Approach	2-13
3	MODEL RESULTS		3-1
	3.1	Model Calibration Approach 1: No-Flow Northern Boundary	3-1
	3.2	Model Calibration Approach 2: Including Caldera Complex	3-6
4	DISCUSSION, CONCLUSIONS, AND RECOMMENDATIONS		4-1
	4.1	Comparison of Results to the U.S. Department of Energy Model	4-1
	4.2	Recommendations	4-1
	4.3	Conclusion	4-2
5	REFERENCES		5-1

FIGURES

Figure		Page
2-1	Map of Structural Features Included in the Flow Model Domain.	2-2
2-2	Satellite Map of the Yucca Mountain Region Showing Flow Model Domain, Interpreted Water Table Elevation Contours Used to Assign Model Boundary.	2-4
2-3	Three-dimensional Oblique View of Model Domain, Looking Northeast	2-6
2-4	Comparison of Cross Sections Along UTM NAD–83 Northing 4069000	2-7
2-5	Cross Section Along UTM NAD–83 Northing 4069000 Showing the Inclusion of Several Fault Zones into the Model Grid.	2-8
3-1	Satellite Map Showing Calculated Hydraulic Head Contours for Flow Model Calibration Following Approach 1	3-2
3-2	Map Showing Constant-Head Contour Lines Calculated for the Approach 1 Flow Model Calibration in Relation to Hydrostratigraphic and Structural Features	3-3
3-3	North-South Cross Section of Calibrated Approach 1 Flow Model Passes Through Well UE–25 p#1 Monitored Interval (Red Square) Just West of Fortymile Wash	3-4
3-4	Plots Showing Relationships Between Observed Hydraulic Heads and Calculated Heads (Upper) and Residual Model Error (Lower) for the Approach 1 Calibrated Model	3-5
3-5	Satellite Map Showing Calculated Hydraulic Head Contours for the Approach 2 Flow Model Calibration	3-8
3-6	Map Showing Constant-Head Contour Lines Calculated for the Approach 2 Flow Model Calibration in Relation to Hydrostratigraphic and Structural Features	3-9
3-7	North-South Cross Section of Calibrated Approach 2 Flow Model Passes Through Well UE–25 p#1 Monitored Interval (Red Square) Just West of Fortymile Wash.	3-10
3-8	Plots Showing Relationships Between Observed Hydraulic Heads and Calculated Heads (Upper) and Residual Model Error (Lower) for the Approach 2 Calibrated Model	3-11

5/22

TABLES

Table		Page
2-1	Major Hydrostratigraphic Layers Used in the Three-Dimensional Flow Model	2-3
3-1	Calibrated Hydraulic Conductivity Values for Approach 1 with No Caldera Complex and a No-Flow Northern Boundary Condition	3-7
3-2	Calibrated Hydraulic Conductivity Values for Approach 2 with Caldera Complex Defined in the Northern Model Region	3-12

6/22

ACKNOWLEDGMENTS

This report was prepared to document work performed by the Center for Nuclear Waste Regulatory Analyses (CNWRA) for the U.S. Nuclear Regulatory Commission (NRC) under Contract No. NRC–02–97–009. The activities reported here were performed on behalf of the NRC Office of Nuclear Material Safety and Safeguards, Division of Waste Management. The report is an independent product of the CNWRA and does not necessarily reflect the views or regulatory position of the NRC.

The authors wish to thank Ron Green for thorough technical review and useful insights, Barbara Long and Cathy Cudd for editorial expertise, and Budhi Sagar for programmatic review. The administrative and format support provided by Arturo Ramos is greatly appreciated.

QUALITY OF DATA, ANALYSES, AND CODE DEVELOPMENT

No original data were generated from the analyses presented in this report. The Grid and MODFLOW modules of the Groundwater Modeling System, Version 3.1, were used to construct and execute the groundwater flow models presented in this report. The Groundwater Modeling System interface and associated codes are presently being validated in accordance with CNWRA operating procedure TOP–18. Documentation of the Groundwater Modeling System modules and demonstration versions of the code can be found at the EMS-i Internet site: http://www.ems-i.com. CNWRA presently maintains two user licenses for Groundwater Modeling System Version 3.1, which contain all codes and documentation. All input and output files for the groundwater flow models presented in this report are archived on a CD-ROM with CNWRA Scientific Notebook 480E; copies may be obtained on request.

A one-time use data-processing algorithm was written to use for reformatting hydrogeologic framework data for Input to the Groundwater Modeling System. Documentation of the data-processing algorithm is also contained in Scientific Notebook 480E.

7/22

1 INTRODUCTION

To evaluate the suitability of Yucca Mountain, Nevada, as a potential nuclear waste repository, the U.S. Department of Energy (DOE) conducts total-system performance assessment analyses to identify important components of natural and engineered barriers to radionuclide transport. The saturated zone beneath Yucca Mountain has been identified as one important component of the natural barrier system. To include saturated zone flow and transport in total-system performance assessment analyses, DOE abstracted flow paths from a site-scale saturated zone flow model. This abstraction is accomplished by using saturated zone flow vectors from a variety of model scenarios in a particle-tracking algorithm to develop unit breakthrough curves.

The U.S. Nuclear Regulatory Commission (NRC) staff, with assistance from Center for Nuclear Waste Regulatory Analyses (CNWRA) staff, are responsible for reviewing the DOE saturated zone process model and total-system performance assessment analyses abstraction to assure that the DOE approach is justified by available data, that data and modeling uncertainties are appropriately considered, and that reasonable alternative conceptual models are considered. As part of this review process, NRC staff also conduct independent total-system performance assessment analyses that include a saturated zone flow path abstraction.

Review of the DOE approach and the development of an independent total-system performance assessment analyses abstraction necessitates an in-depth understanding of saturated zone hydrogeology at Yucca Mountain and a means to independently evaluate model and data uncertainties and potentially important alternative conceptual models for saturated zone flow. To this end, CNWRA staff are developing a three-dimensional groundwater flow model of the Yucca Mountain, Nevada, region. The foundation of this flow model is the CNWRA hydrogeologic framework model (Sims, et al., 1999), which was also developed independently from the DOE model. The insights gained through such independent model development are very useful for a risk-informed review of DOE models. Because the CNWRA flow model is based on a substantially different hydrogeologic framework model compared with the DOE model, the CNWRA flow model provides a means for evaluating the sensitivity of simulated flow paths to the underlying interpretation of geologic structure. The CNWRA flow model also provides NRC and CNWRA staff with a tool to evaluate alternative conceptualizations of how particular hydrogeologic features may affect calculated flow paths in the saturated zone. Finally, this flow model can also be used to quantify data and model uncertainty in the saturated zone flow path abstraction for the NRC performance assessment tool.

This letter report documents the conceptual approach and progress of development of this independent flow model for NRC review.

2 MODEL DESCRIPTION AND APPROACH

The MODFLOW modular finite-difference groundwater flow modeling code (Harbaugh and McDonald, 1996) was used for the flow calculations presented in this report. The following sections provide descriptions of the modeling assumptions and limitations, the hydrogeologic framework, model grid development, hydrologic properties, boundary conditions, and calibration approach.

2.1 Model Assumptions and Limitations

The MODFLOW code allows consideration of either confined or unconfined aquifer conditions, or a combination of the two. Only the confined aquifer solution is used for the analyses presented in this report. Additional MODFLOW calculation tools include separate modules for considering distributed water table recharge, evapotranspiration, well pumping or injection, river recharge, and general-head boundary conditions. None of these additional modules are used for the analyses presented in this report. Although distributed water table recharge and well pumping are active processes within portions of the model region, the quantity of water involved in these processes is small compared to lateral flow into and out of the model side boundaries. Recharge and well pumping can be easily included in future analyses.

Heterogeneity in groundwater flow system properties is considered in the three-dimensional site-scale model by assigning different hydrologic properties to the different hydrostratigraphic layers and structural features included in the model. Within any particular layer or structural feature, however, hydrologic properties are assumed to be homogenous.

The MODFLOW code allows consideration of horizontal and vertical anisotropy in hydraulic conductivity, with the limitation that the principal axes of anisotropy must be aligned with the model grid. Only isotropic hydrologic properties are assumed for the model developed in this report. Effects of horizontally and vertically anisotropic hydraulic conductivity can be evaluated in future analyses.

2.2 Hydrogeologic Framework

The foundation for assigning material types to the groundwater flow model is the CNWRA Hydrogeologic Framework Model (Sims, et al., 1999). The Hydrogeologic Framework Model defines layer boundaries and structural features based on interpretations of available borehole and geophysical data. The structural features adapted from the Hydrogeologic Framework Model for the flow model are shown in Figure 2-1. The six Hydrogeologic Framework Model hydrostratigraphic layers used in the model are listed and described in Table 2-1. These layers generally correspond to the major hydrostratigraphic units described by Luckey, et al. (1996).

2.3 Model Domain and Grid

The finite-difference numerical grid for the three-dimensional site-scale flow model of Yucca Mountain was created using the GRID module of Groundwater Modeling System, Version 3.1 (Environmental Modeling Research Laboratory, 1999).

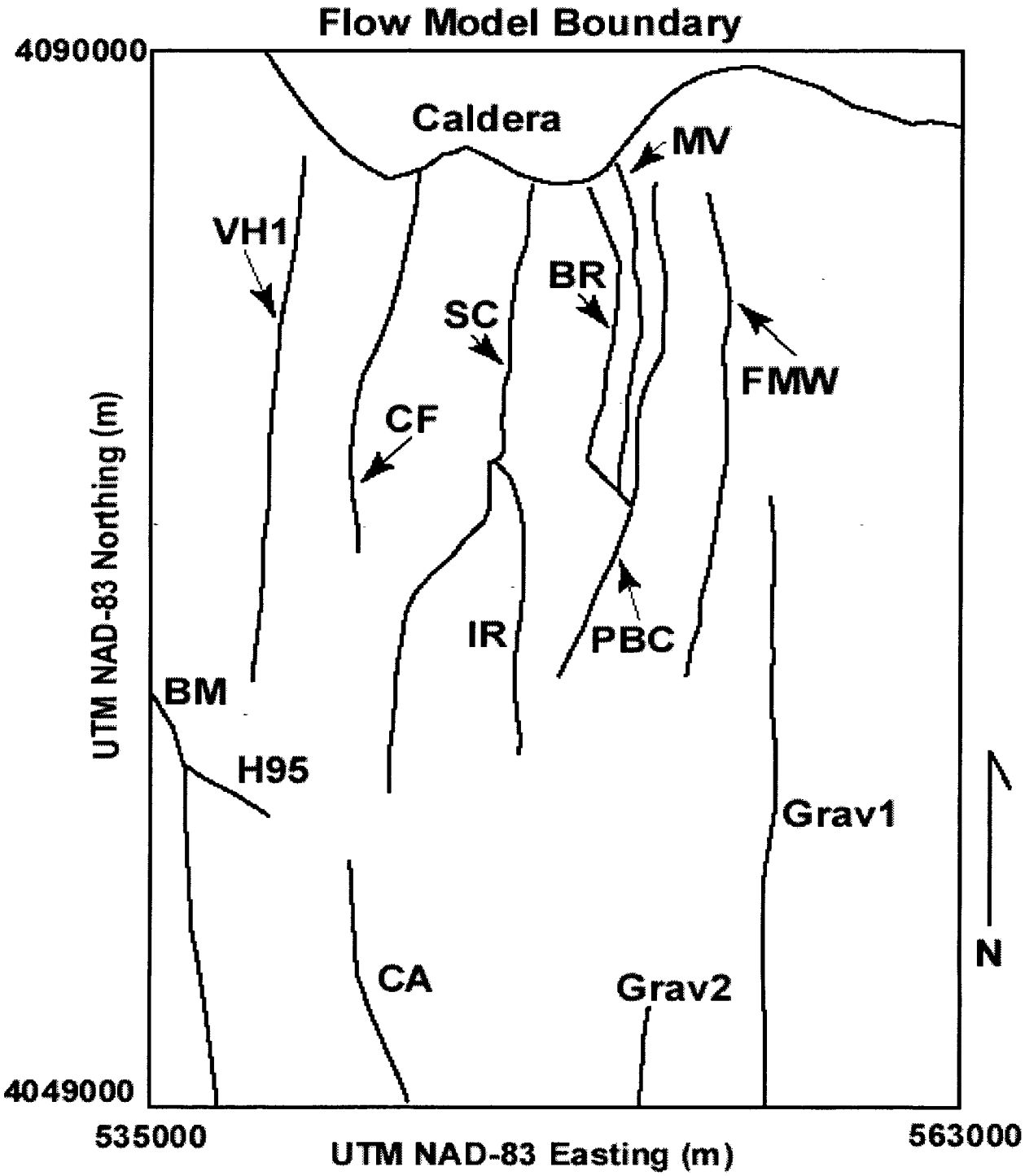

Figure 2-1. Map of Structural Features Included in the Flow Model Domain: Timber Mountain Caldera Complex (Caldera), Bare Mountain Fault (BM), Solitario Canyon Fault (SC), Iron Ridge Fault (IR), Crater Flat Fault (CF), VH-1 Fault , Fortymile Wash Fault (FMW), Bow Ridge Fault (BR), Midway Valley Fault (MV), Paintbrush Canyon Fault (PBC), Central Amargosa Fault (CA), Highway 95 Fault (H95) and Two Faults Inferred From Gravity Data (Grav1 and Grav2)

9/22

Table 2-1. Major Hydrostratigraphic Layers Used in the Three-Dimensional Flow Model		
Material Type Designation for Major Hydrostratigraphic Layers in Three-Dimensional Flow Model	**Sims, et al. (1999) Layer Designation**	**Description of Included Lithologic Units**
Alluvium	topo	Valley-fill sediments, including lacustrine, debris-flow, stream-channel, and overbank deposits
Upper Volcanic Aquifer	tiva	Timber Mountain and Paintbrush groups: from top of the Tiva–Rainier Tuff to top of the Calico Hills Tuff; a major subunit is the Topopah Springs Tuff
Upper Volcanic Confining Unit Layer	calico	Calico Hills Formation
Lower Volcanic Aquifer	prow	Grater Flat Group: major subunits include the Prow Pass, Bullfrog, and Tram Tuffs
Lower Volcanic Confining Layer	tund	Lithic Ridge and older Tuffs
Regional Paleozoic Aquifer	top_Pz	Paleozoic-age rocks: predominantly carbonates (limestones and dolomites) and other sedimentary rocks (shales, siltstones, and sandstones)

The first consideration for selection of the model domain was to center the model around potential flow paths from Yucca Mountain to the 18-km [11.2-mi] compliance boundary. In deciding the lateral and vertical extents of the model, it was necessary to strike a balance between keeping the computational grid small enough to achieve reasonable model run times and large enough so the model boundaries are far enough from the area of interest (i.e., potential flow paths) to mitigate the error caused by uncertainty in model boundary conditions.

The rectangular lateral boundaries of the model domain are shown on a satellite map in Figure 2-2. Using the UTM NAD–83 coordinate system, the southwest corner of the model occurs at Easting 535000, Northing 4049000. The northeast corner occurs at Easting 563000, Northing 4090000. The model domain thus covers a 28 × 41-km [17.4 × 25.5-mi] area. The bottom of the three-dimensional model domain is at a constant elevation of 1,500 m [4,920 ft] below sea level. The top of the model domain occurs at 1,200 m [3,936 ft] above sea level; however, all of the model grid cells that are entirely above the water table elevation were flagged as inactive. The water table elevation used to identify inactive cells is based on an interpretation by Winterle, et al. (2000, Figure 4-1). The water table elevation contours shown in Figure 2-2 reflect a more recent interpretation used as the basis for assigning constant-head values to the model side boundaries. The model grid is horizontally discretized using 300-m

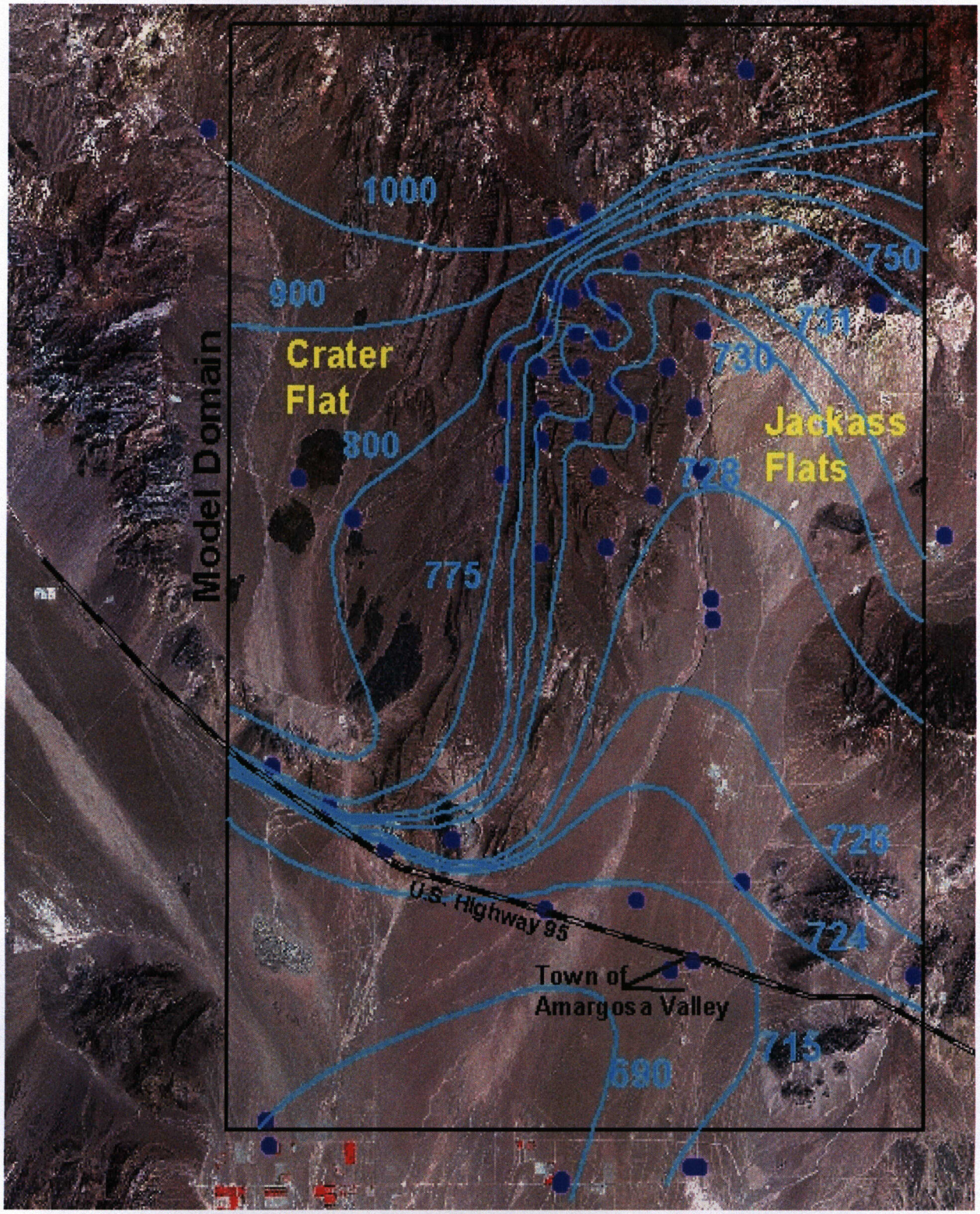

Figure 2-2. Satellite Map of the Yucca Mountain Region Showing Flow Model Domain, Interpreted Water Table Elevation Contours Used to Assign Model Boundary Conditions, and Locations of Wells Used to Interpret the Water Table

[984-ft] square grid blocks. A limitation that results from this horizontal discretization is that the minimum fault-zone width that can be considered in the model is 300 m [984 ft]. As will be seen in the model results, the fault zones in the model grid are sufficient to reproduce the steep hydraulic gradients across the Solitario Canyon and Highway-95 fault zones. Note that the DOE saturated zone flow model uses a 500-m [1,640-ft] square horizontal grid discretization. Vertical grid cell thickness varies between 50 and 200 m [164 and 656 ft]. The 50-m [164-ft] thickness is assigned to cells with elevations between 200 and 900 m [656 and 2,953 ft] above sea level, so that the finest discretization coincides with the potential transport pathways away from Yucca Mountain. The resulting numerical grid contains 138 × 95 × 30 cells in the north-south, east-west, and vertical dimensions. In Figure 2-3, a three-dimensional oblique view of the active numerical grid shows the horizontal and vertical discretizations, and illustrates how the uppermost active cells follow the water table elevation.

2.4 Incorporation of Layer and Structural Features in the Model Grid

To assign material properties to the MODFLOW model grid, a data processing algorithm[1] was used to determine which hydrostratigraphic unit in the Hydrogeologic Framework Model is assigned at the location of the center of each flow model grid block and to format this information as input for the Groundwater Modeling System grid-building interface. Figures 2-4a and 2-4b show a comparison of cross sections from the Hydrogeologic Framework Model and from the flow model after material properties were assigned using this algorithm. It can be seen that the Hydrogeologic Framework Model hydrostratigraphic units are properly assigned to the flow model, except that the Upper Volcanic Confining layer is discontinuous in some areas of the flow model grid. This problem with the Upper Volcanic Confining layer occurs when it is thinner than the model grid thickness and passes through a grid cell without intersecting the cell center. Refinement of the flow model to thinner grid cells would help solve this problem, but would render the model too computationally cumbersome. It is important to capture the continuity of the Upper Volcanic Confining layer because confining or semiconfining layers, even when thin, can significantly affect groundwater flow directions. To make the Upper Volcanic Confining layer continuous, the material properties assigned to the model grid were edited manually, using the graphical Groundwater Modeling System grid interface. Editing resulted in the Upper Volcanic Confining layer being thicker in the lower portion of the model grid compared to the predicted layer thickness in the hydrogeologic framework model (Figure 2-4c). In the area of interest near the water table, however, the potential bias of increased thickness of the Upper Volcanic Confining layer is within the range of uncertainty of layer thickness in the hydrogeologic framework model.

Structural features were also added to the model grid by manually selecting the pertinent grid cells and identifying them as separate features in the model. Several east-west cross sections from the hydrogeologic framework model were printed and used to visually aid selection of the appropriate grid cells for each fault. The widths of fault zones in the model were generally the width of a single grid cell, but where fault planes curve or dip, a width of two grid cells was sometimes used to maintain fault zone continuity. Additionally, because of the close proximity of the Bow Ridge, Midway Valley, and Paintbrush Canyon faults, the entire area between these faults is treated as a single fault zone. Figure 2-5 shows the same flow-model cross section from Figure 2-4 following the inclusion of fault zones.

---

[1]Documented in CNWRA Scientific notebook 480E.

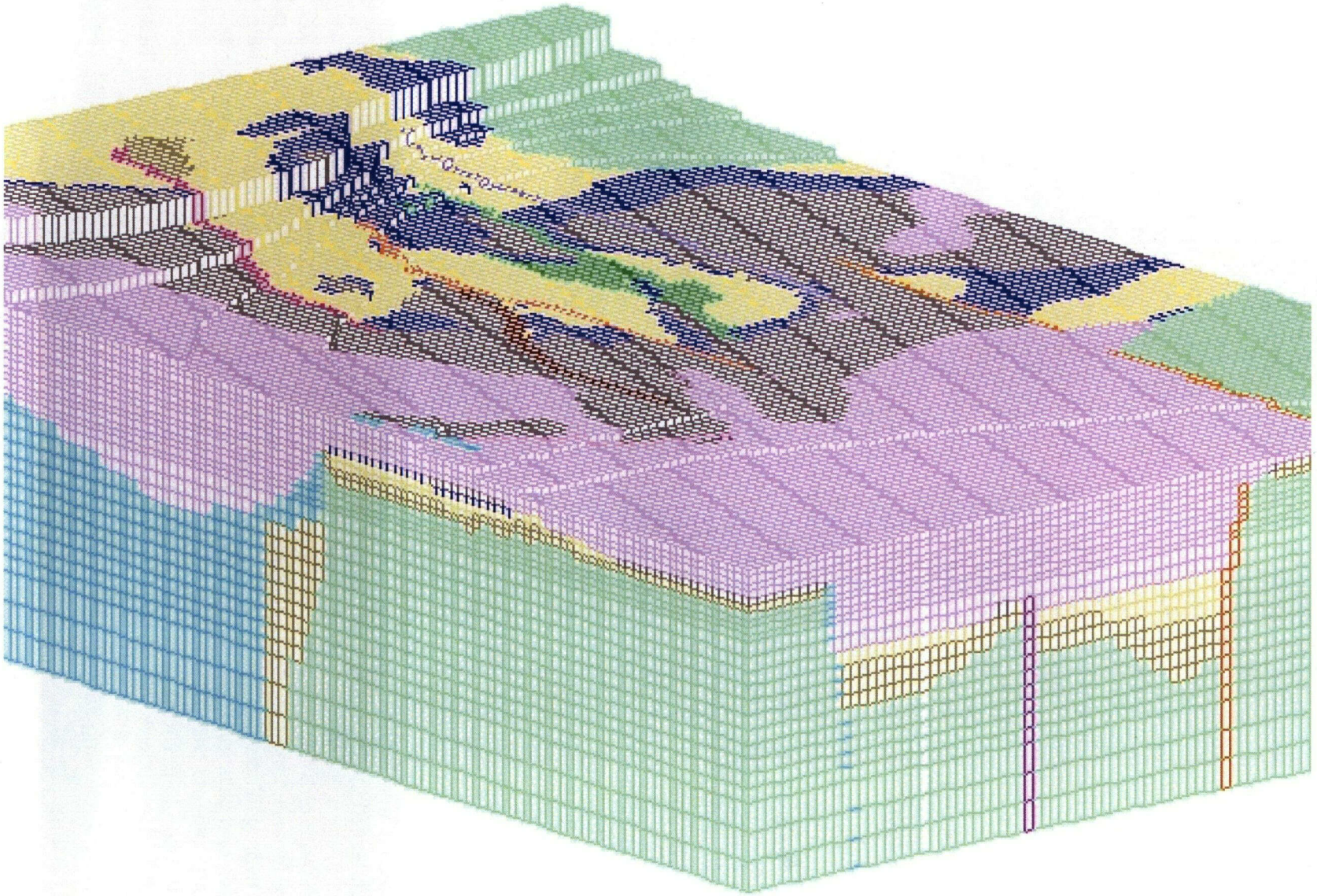

Figure 2-3. Three-Dimensional Oblique View of Model Domain, Looking Northeast

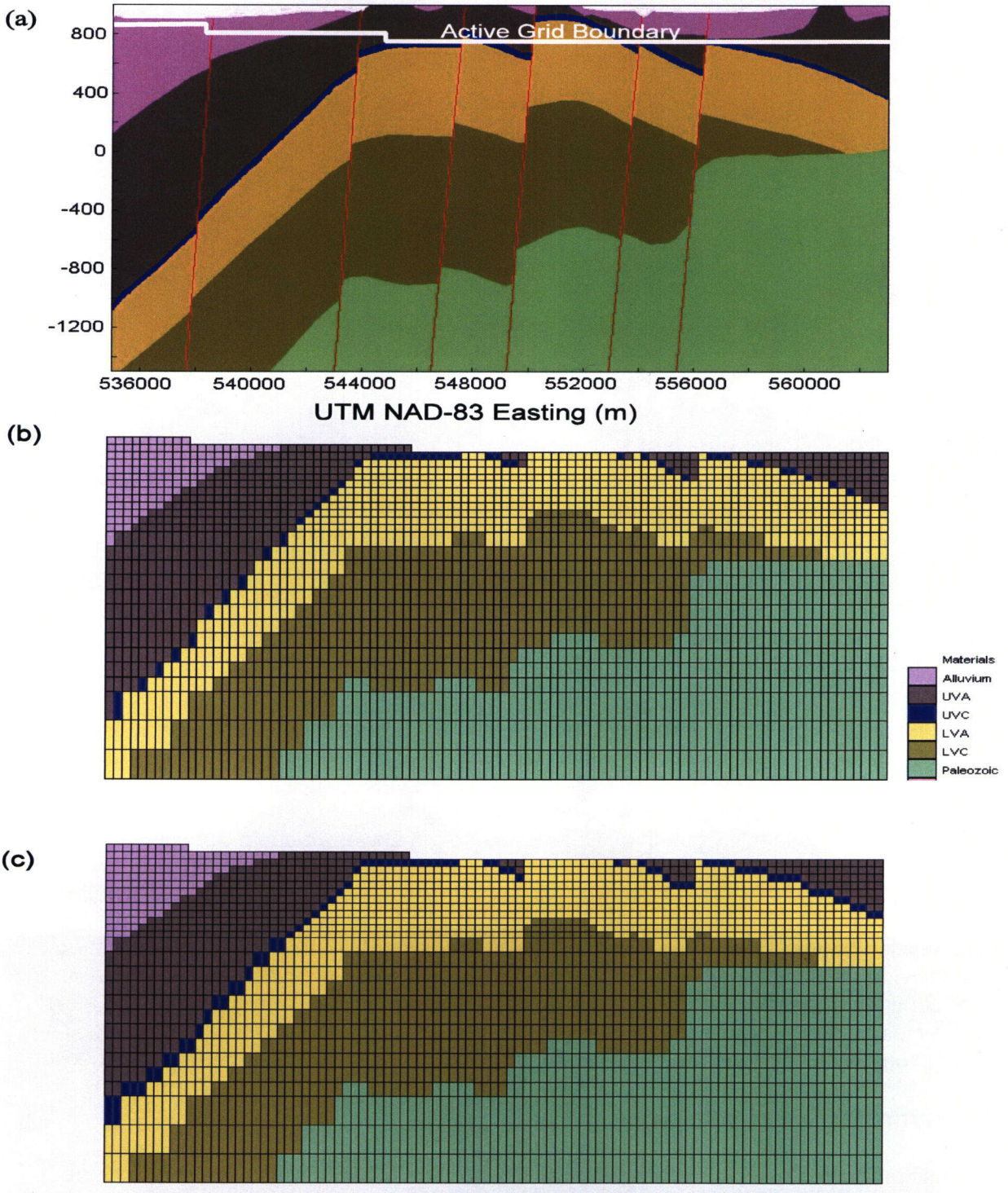

Figure 2-4. Comparison of Cross Sections Along UTM NAD–83 Northing 4069000 from (a) the Hydrogeologic Framework Model of Sims, et al. (1999), (b) the Initial Flow Model Grid Showing Materials Assigned by the Gridding Algorithm, and (c) the Model Grid After Manually Editing the Upper Volcanic Confining Layer (Blue) Where It Was Missed by the Algorithm

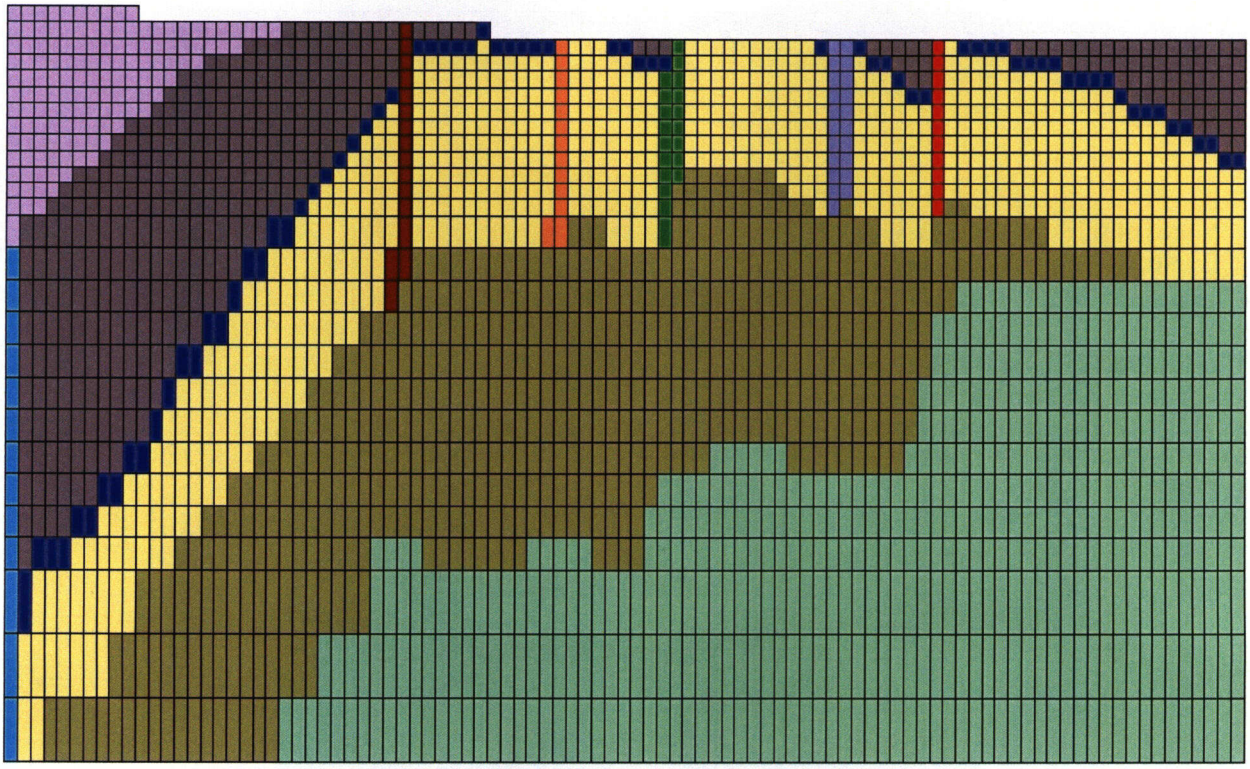

Figure 2-5. Cross Section Along UTM NAD–83 Northing 4069000 Showing the Inclusion of Several Fault Zones into the Model Grid

Notice in Figure 2-5 that the downward extent of several faults is terminated at the top Lower Volcanic Confining layer, whereas the faults are shown as continuous with depth in the hydrogeologic framework model. This parsimonious approach to assigning fault properties was taken because there is no evidence available to infer hydrologic properties of faults within or beneath the Lower Volcanic Confining layer. Because the Lower Volcanic Confining layer is already conceptualized as a low-permeability layer, assigning fault features of similar low permeability in this layer would not likely affect model results. The converse possibility exists that faults within the Lower Volcanic Confining layer could act as conduits for hydraulic communication between the Paleozoic Aquifer and the Lower Volcanic Aquifer. The limited available evidence suggests, however, that the Lower Volcanic Confining layer provides good vertical confinement, even in the vicinity of fault zones (e.g., Painter, et al., 2002). The effects of fault zones on model results is discussed in greater detail in Section 3.0 of this report. The hydrologic properties assigned to layers and fault zones are discussed in the following section.

2.5 Hydrologic Properties

Hydrologic properties used in confined aquifer solution for MODFLOW calculations include transmissivity, vertical conductance, horizontal anisotropy ratio, and specific storage. Because only steady-state flow conditions are examined in this report, changes in water storage are not considered, and the specific storage coefficient is not used. As previously mentioned, horizontal anisotropy is not considered for this initial model development; hence, a horizontal anisotropy ratio of 1.0 is assumed for all layers and structural features. The MODFLOW

graphical preprocessor of the Groundwater Modeling System interface calculates layer transmissivity and vertical conductance automatically for each grid cell based on user inputs of horizontal and vertical hydraulic conductivities and grid cell thickness. Because the model boundary conditions and grid dimensions are fixed for the analyses in this report, hydraulic conductivity for each layer and structural feature is the variable parameter that determines the calculated three-dimensional distribution of hydraulic heads. The following sections provide a general discussion of available information for considering constraints on the hydraulic conductivity assigned to layers and structural features.

2.5.1 Hydrostratigraphic Layers

Hydraulic conductivity values assigned to model layers can be estimated from hydraulic test data collected from Yucca Mountain area wells. For some layers, however, hydraulic test data are limited. For example, published hydraulic test data are available from only a single well in the Paleozoic Aquifer. It is, therefore, useful to also consider more qualitative sources of data, such as the distribution of hydraulic heads and the aquifer pressure response to earth-tide induced strain. Rationale is given in the following paragraphs for initial estimates of hydraulic conductivity for each of the six hydrostratigraphic layers.

Alluvium

Large areas of saturated valley-fill alluvium exist within the modeled region in Crater Flat to the west and in the Amargosa Valley to the south. The deposition of valley-fill sediments occurs from a variety of morphologic processes. Hence, the hydrologic properties of alluvium are expected to be spatially heterogenous. For initial development of the models presented in this report, however, spatial heterogeneity in saturated alluvium is not considered. Hydrologic properties of alluvium in the southern portion of the modeled region are of greatest interest because this area contains possible flow paths from Yucca Mountain. Aquifer pumping tests have been conducted in several wells completed in alluvium as part of the Nye County Early Warning Drilling Program. Preliminary results, based on presentations made by Nye County researchers, from these pumping tests indicate hydraulic conductivity on the order of 1–10 m/d [25–250 gal/d/ft^2]. DOE is expected to provide additional analyses of the hydrologic and hydrostratigraphic properties of the alluvial sediments on completion of the Early Warning Drilling Program studies and the ongoing interwell hydraulic and tracer studies at the Alluvial Testing Complex.

Upper Volcanic Aquifer

The Upper Volcanic Aquifer comprises layers of highly fractured welded tuffs of the Topopah Springs and Tiva Canyon formations. Air permeability tests conducted in the unsaturated portion of these formations indicate permeability on the order of 10^{-11} to 10^{-12} m^2 [1 to 10 darcy] (e.g., LeCain, 1998; LeCain, et al., 1999), which translates to a hydraulic conductivity range of about 1–10 m/d [25–250 gal/d/ft^2]. Saturated hydraulic test data for this model layer is available from Wells J–13 and JF–3 in the Fortymile Wash area. Testing in well J–13 (Thordarson, 1983) indicates a hydraulic conductivity on the order 1 m/d [25 gal/d/ft^2]. Testing in Well JF–3 (Plume and La Camera, 1996) showed an anomalously high hydraulic conductivity, in excess of 100 m/d [2,500 gal/d/ft^2]. The high hydraulic conductivity in Well JF–3

may be the result of its proximity to a discrete high-permeability feature, perhaps the Fortymile Wash fault.

Upper Volcanic Confining Layer

The Upper Volcanic Confining layer consists of the nonwelded tuffs of the Calico Hills formation and nonwelded portions of the upper Prow Pass unit of the Crater Flat Formation. The Upper Volcanic Confining layer separates the Upper and Lower Volcanic Aquifers. Hydraulic test data for this layer are available from numerous wells in the Yucca Mountain area (e.g., see reviews by Luckey, et al., 1996 and Geldon, 1993) and indicate permeability for this layer is generally lower than the overlying and underlying Upper and Lower Volcanic Aquifers. The characterization of this layer as a confining unit can be misleading, however, as flow meter surveys in some wells show this layer to be moderately productive. For example, this layer accounted for approximately 1–5 percent of water production in the C-Holes tests (Geldon, 1993). Hydraulic conductivity for this layer is estimated in the range 0.01–0.1 m/d [0.25–2.5 gal/d/ft^2], which is generally consistent with the range estimated from hydraulic tests (e.g., CRWMS M&O, 2000, Figure 15).

Lower Volcanic Aquifer

The Lower Volcanic Aquifer consists of most of the Prow Pass unit, the entire Bullfrog unit, and the upper part of the Tram unit of the Crater Flat Formation. Pumping test data for this layer, available from numerous wells in the Yucca Mountain area, consistently indicate hydraulic conductivity within a range of approximately 0.1 to 1 m/d [2.5–25 gal/d/ft^2](e.g., CRWMS M&O, 2000, Figure 15). Values of hydraulic conductivity for the Lower Volcanic Aquifer estimated from the C-Holes tests are generally higher than this range (e.g., Geldon, et al., 1998 and Winterle and La Femina, 1999). The area tested by the C-Holes, however, lies between the Bow Ridge and Paintbrush faults, which is treated as a fault zone in this model and assigned a separate hydraulic conductivity (Section 2.5.2).

Lower Volcanic Confining Layer

The Lower Volcanic Confining layer consists of the Lithic Ridge Tuff and the underlying thick sequence of older unnamed ash-flow tuffs. There are few data available to estimate a bulk hydraulic conductivity for this layer. Available evidence does indicate, however, that this thick sequence of generally nonwelded tuffs acts as an areally continuous low-permeability confining layer. This evidence includes the pronounced earth-tide response in well water levels beneath or in the lower portions of this layer. Well-bore flow meter surveys in several wells consistently reveal a zone, typically several hundred meters thick, that does not contribute detectable quantities of water to well production. Additionally, hydraulic heads beneath or in the lower portions of the Lower Volcanic Confining layer are several to tens of meters greater than the heads in the overlying Lower Volcanic Aquifer. For initial modeling purposes, an arbitrary estimate for hydraulic conductivity is 10^{-5} m/d [2.5×10^{-4} gal/d/ft^2], which is generally consistent with the range used by CRWMS M&O (2000, Figure 15).

Paleozoic Aquifer

Hydraulic testing data are available for the Paleozoic Aquifer from only one well, UE–25 p#1 (p#1). Testing in p#1 (Craig and Robison, 1984) indicates a modest hydraulic conductivity on

the order of 0.1 m/d [2.5 gal/d/ft^2]. This single data point represents only a small area in the uppermost portion of the Paleozoic Aquifer, whereas the Paleozoic Aquifer layer occupies more than half the entire volume of the model domain and extends to depths much deeper than any well in the model area. Thus, there is a significant uncertainty in the appropriate value assigned to the hydraulic conductivity of the Paleozoic Aquifer.

2.5.2 Faults

Several of the faults included in the model have been directly observed and mapped from surface outcrops. Other faults have been neither mapped at the surface nor recorded in well logs, but are inferred from gravity or other geophysical data. Little is known about the hydrologic properties of the faults in the model area or how fault properties might change with depth. Fault zone characteristics that might affect hydrogeologic properties include width of the damage zone created by the fault, chemical and physical alteration of rock properties within the fault zone, amount of fault displacement, and zones of increased fracturing adjacent to or between fault zones. In some cases generalized fault hydrologic properties can be inferred from other observations, such as when changes in the hydraulic gradient are aligned with a particular fault zone. Rationale for assigning initial hydraulic conductivity values to specific faults is discussed in the following paragraphs.

Bow Ridge—Paintbrush Canyon Fault Zone

The Bow Ridge—Paintbrush Canyon fault zone is conceptualized as a zone of increased fracturing in the Upper and Lower Volcanic Aquifers between the Bow Ridge and Paintbrush Canyon faults, including the Midway Valley fault. This zone, which is as much as 2.4 km [1.5 mi] wide, represents much of the aquifer volume tested during the long-term pumping test at the C-Holes testing complex. In that regard, the Bow Ridge—Paintbrush Canyon zone is generally analogous to a feature in the DOE flow model referred to as the Imbricate Fault Zone (CRWMS M&O, 2000). Test data from the C-Holes indicate hydraulic conductivity in this area is on the order of 1–10 m/d [25–250 gal/d/ft^2] (e.g., Geldon, et al., 1998 and Winterle and La Femina, 1999).

Solitario Canyon and Iron Ridge Faults

The north-south trending Solitario Canyon-Iron Ridge fault system is coincident with the moderately high hydraulic gradient beneath the west side of Yucca Mountain. There are no test data available from which to form a reliable estimate for the hydraulic conductivity of this fault zone. Hence, the Solitario Canyon and Iron Ridge and the western splay of the Solitario Canyon fault (SC_west) are conceptualized as low-permeability structural features. The hydraulic conductivity values assigned to these features for analyses in this report are based on manual calibrations to reproduce the observed hydraulic gradient.

Highway–95 Fault

The Highway–95 fault is a splay off the Bare Mountain fault that generally strikes in the direction of U.S. Highway 95. There is no significant vertical offset associated with this fault, but there is a moderately high hydraulic gradient across the fault that indicates a zone of reduced permeability. The hydraulic conductivity value assigned to the Highway–95 fault in the analyses

presented in this report is based on manual calibrations to reproduce the observed hydraulic gradient.

Fortymile Wash Fault

The Fortymile Wash fault, as the name implies, underlies Fortymile Wash. There are no outcrop data to confirm the existence of this fault. Hydrologic properties are unknown, except that the conceptualization of the Fortymile Wash fault as a high-permeability feature provides a possible explanation for the anomalously high permeability estimated for Well JF–3. A somewhat arbitrary hydraulic conductivity value of 10 m/d [250 gal/d/ft^2] is assigned to this fault for the analyses presented in this report. The uncertainty in the geometry and hydrologic properties of this fault zone should be evaluated in future analyses because the fault lies along potential flow paths from Yucca Mountain.

Bare Mountain Fault

The Bare Mountain fault is a major structural feature with vertical offset exceeding 1 km [0.62 mi] within the model region. There are no data available from which to estimate hydraulic properties of this fault. Because of the large offset, however, it is conceptualized that cross-fault permeability may be reduced by a resulting fine-grained fault core. In the hydrogeologic framework model, the majority of this fault lies just outside the western boundary of the flow model. The western boundary of the flow model, however, is assigned Bare Mountain fault properties in areas where Bare Mountain fault is just outside the model domain to allow the ability to account for potential effects of this fault on groundwater flux across the western model boundary. A value of 0.001 m/d [0.025 gal/d/ft^2] is assigned to the Bare Mountain fault for the analyses presented in this report to approximate reduced permeability of the fault gouge often associated with such large-offset faults.

Crater Flat and VH–1 Faults

The Crater Flat and VH–1 faults are both situated beneath Crater Flat to the west of Yucca Mountain. The hydrologic properties of these two faults are unknown. They were arbitrarily assigned hydraulic conductivity values of 0.001 m/d [0.025 gal/d/ft^2] for initial model development based on scoping model predictions.

Central Amargosa and Gravity Faults

The Central Amargosa fault and two Gravity faults (Grav1 and Grav2) are located in Amargosa Valley in the southern portion of the model. Hydrologic properties of these faults are unknown, hence, they were assigned hydraulic conductivity values of 1.0 m/d [25 gal/d/ft^2] for initial model development based on scoping model predictions. For the second of two model calibration approaches described in Chapter 3, hydraulic conductivity for the Grav1 fault was reduced to 0.1 m/d [2.5 gal/d/ft^2].

2.5.3 Caldera Complex

Interpretation of the caldera complex boundary shown in Figure 2-1 is taken from the hydrogeologic framework model (Sims, et al., 1999). Within the caldera complex boundary, the

possibility of substantial alteration of hydrologic properties within layers must be considered. The presence of this caldera complex is problematic for model development for two reasons. First, the boundary for the caldera shown in Figure 2-1 represents an approximate best guess based on limited data.[2] Second, there are no data or analyses that can be used to determine the hydrologic properties of layers within the caldera complex. Available data from wells suggest that water levels in the northern portion of the model area are 200 to 300 m [650 to 1,000 ft] higher than in the rest of the model. The rapid northward increase in water levels in this area suggests the caldera region may represent a barrier to flow or that water level measurements in this area represent perched water. In the two models presented in Chapter 3 of this report, two approaches were taken to consider possible effects of the caldera complex area on groundwater flow. In the first approach, the caldera zone is not explicitly included in the model, but a no-flow northern boundary is used to evaluate the caldera zone as a barrier to flow. In the second model approach, the caldera is explicitly represented by introducing two new material types—one to represent alteration of volcanic rocks (Caldera_VR) and one to represent alteration of Paleozoic rocks (Caldera_PZ). Delineation of the caldera zone in the flow model was based on judgment regarding where zones of alteration were necessary to improve model calibration. Thus, the geometry of the caldera zone in the flow model does not necessarily conform to the caldera geometry in the hydrogeologic framework model. The hydraulic conductivity assigned to these material types was established through manual model calibration.

2.6 Boundary Conditions

The model was assigned no-flow top and bottom boundary conditions. Constant heads were specified on the model side boundaries. Constant head values specified for the side boundaries were based on the interpretation of the water table elevation depicted in Figure 2-2. A constant head of 1,100 m [3,608 ft] was selected for the entire northern boundary based on the conceptualization that the highest water table elevations in the northern model area reflect perched water.

The hydraulic head values assigned to the side boundaries were assumed to remain constant with depth. That is, the same interpolated hydraulic head value assigned to an uppermost active boundary cell was assigned to all vertically underlying cells. This major assumption likely introduces some error into the model. It is hoped that the area of interest in the center of the model domain is far enough from the model boundaries that calculated vertical gradients are not biased by this model uncertainty. Possible effects of vertical gradients at the model boundaries are beyond the scope of this initial analysis, but should be evaluated in future analyses—especially considering that the same assumption is made in the DOE saturated zone flow model.

2.7 Model Calibration Approach

Results presented in Chapter 3 of this report are based on a manual trial-and-error calibration process. Hydraulic conductivity values were varied for each of the 6 hydrostratigraphic layers and 13 structural features included in the model to obtain a reasonable match to hydraulic

---

[2]Sims, D. Personal communication (January 23) to J. Winterle, CNWRA. San Antonio, Texas: CNWRA. 2002.

heads observed in area wells. Particular importance was placed on achieving a good calibration where water table elevations are between 750 and 715 m [2,460 and 2,345 ft], which is the area of the flow paths from Yucca Mountain to potential receptor locations in Amargosa Valley. Emphasis was also placed on reproducing the observed upward hydraulic gradient between the Paleozoic and the Lower Volcanic Aquifers at Well UE–25 p#1, where the observed hydraulic head is approximately 753 m [2,620 ft] in the Paleozoic Aquifer and approximately 730 m [2,540 ft] in the Lower Volcanic Aquifer (Graves, 2000).

Inverse optimization tools can be applied to MODFLOW models through the groundwater modeling system interface. Given the large model size, however, the number of parameters that would need to be optimized would be computationally prohibitive without first obtaining an approximate model calibration and constraints on parameter values. Inverse optimization methods will be employed in future analyses that will benefit from the insights gained in model development presented in this report. Note that the DOE Flow Model is calibrated using the PEST, Version 2.0, parameter estimated code.

It should be noted that, for this steady state-model calibration with constant head side boundary conditions, calibration does not depend on the set of *absolute* values of hydraulic conductivity assigned to the model material types. Rather, calibration is driven by the *relative* hydraulic conductivity of each material type compared to the other material types. For example, if a set of hydraulic conductivity values is determined to produce a reasonable calibration, one could multiply the set of values by any constant value and obtain the same model calibration. Thus, unless the hydraulic conductivity value for at least one material type is held constant, one cannot obtain a unique calibrated property set. For the simulations discussed in the following Chapter, the value for the Lower Volcanic Aquifer is held constant at 0.1 m/d [2.5 gal/d/ft^2]; thus, the uncertainty in the Lower Volcanic Aquifer hydraulic conductivity extends to the entire calibrated property set.

15/32

3 MODEL RESULTS

An attempt to calibrate the flow model was made using an approach that included only the hydrogeologic framework model hydrostratigraphy without any structural features. It quickly became evident, however, that a reasonable calibration could not be obtained without including certain faults. In particular, the Solitario Canyon-Iron Ridge fault system and the Highway-95 fault were necessary to reproduce the high hydraulic gradients coincident with these faults. All subsequent models included reduced hydraulic conductivity assigned to these faults.

It was observed, after including in the model all the faults shown in Figure 2-1, that some type of reduced permeability zone or barrier to flow in the area of the caldera complex would be necessary for model calibration. Without such a barrier, high heads from the constant-head northern boundary condition propagate southward deep into the model through the Lower Volcanic Aquifer. DOE experienced similar results in its saturated zone model and solved the problem by introducing an east-west-trending barrier across the entire model in the area of the high hydraulic gradient north of Yucca Mountain (CRWMS M&O, 2000). For the model presented in this report, two approaches to treat the area of the caldera complex were examined. First, the northern boundary of the model was changed to a no-flow boundary. The second approach was to explicitly define two new material types for volcanic and Paleozoic rocks in the northern portion of the model to represent alteration of hydrologic properties within the caldera zone, as described in Section 2.5.2. Model results for these two approaches are given in the following two sections.

3.1 Model Calibration Approach 1: No-Flow Northern Boundary

The first approach for model calibration included all model layers and structural features as described in Section 2.5, except for material properties associated with the caldera complex. As previously discussed, reasonable calibration could only be obtained for this model by assigning a no-flow boundary condition to the northern boundary.

Hydraulic heads calculated for grid layer 7 of the Approach 1 calibrated model are illustrated in the contour map in Figure 3-1. Layer 7 is used for illustrative purposes because it is the uppermost layer that covers the entire lateral extent of the model domain. In the area of interest for flow paths from Yucca Mountain, Figure 3-1 generally compares favorably to the water table elevation map in Figure 2-2.

To illustrate the effects of structure and layering on the distribution of hydraulic heads, calculated head contour lines are again plotted for grid layer 7 in Figure 3-2 on a map showing material types. The importance of the Solitario Canyon-Iron Ridge and Highway-95 faults for reproducing the steep hydraulic gradients in their respective areas is evident in Figure 3-2.

Figure 3-3 is a north-south cross section that passes through the location of Well p#1. The red square in Figure 3-3 indicates the location of the monitored interval in Well p#1. Note that the upward hydraulic gradient across the Lower Volcanic Confining layer is reproduced, but the magnitude of the vertical head difference predicted across the Lower Volcanic Confining layer is only 8.6 m [28.2 ft], compared to the 23-m [75-ft] head difference observed in p#1.

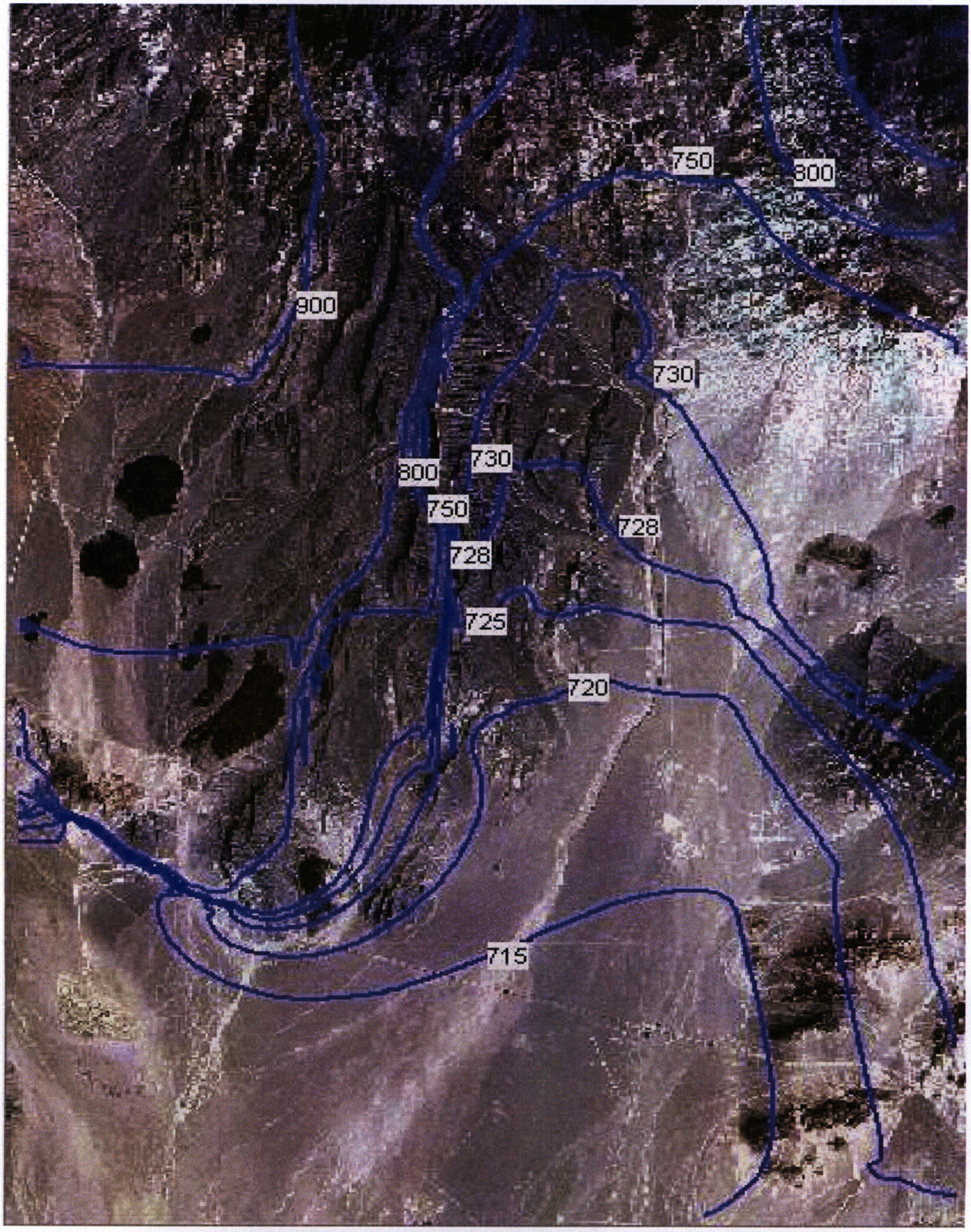

Figure 3-1. Satellite Map Showing Calculated Hydraulic Head Contours for Flow Model Calibration Following Approach 1

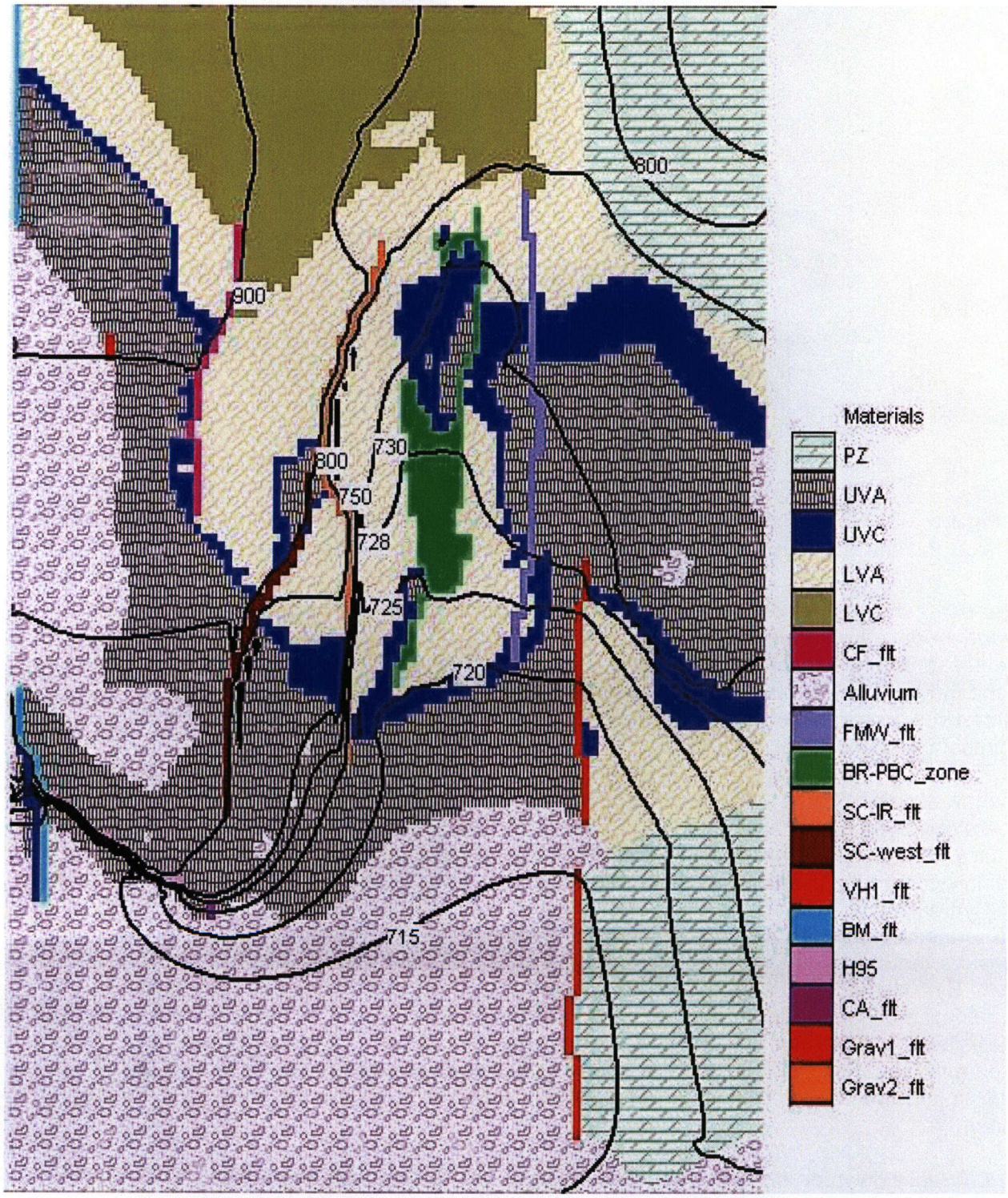

Figure 3-2. Map Showing Constant-Head Contour Lines Calculated for the Approach 1 Flow Model Calibration in Relation to Hydrostratigraphic and Structural Features (see Table 3-1 for material designations in legend)

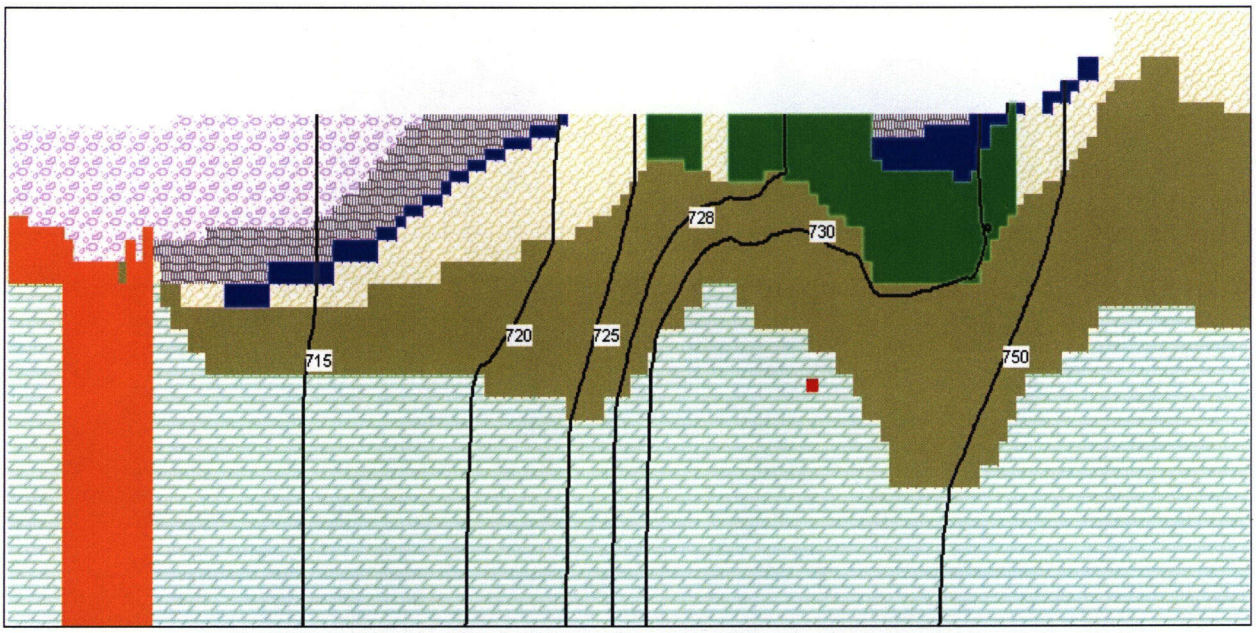

Figure 3-3. North-South Cross Section of Calibrated Approach 1 Flow Model Passes Through Well UE–25 p#1 Monitored Interval (Red Square), Just West of Fortymile Wash

Figure 3-4 shows plots comparing hydraulic heads observed in area wells to heads calculated by the model (upper plot) and to residual errors in the calculated head (lower plot). The greatest differences between calculated and observed head values occur in the northern region of the model where observed heads are greater than 800 m [2,624 ft]. Some of these differences are explained by the conceptualization that the highest heads in the northern area represent perched water.

The lower plot in Figure 3-4 focuses on residual errors in the area of interest in the model where observed heads are below 800 m [2,624 ft]. The greatest residual errors in this plot occur where observed heads are greater than approximately 775 m [2,542 ft]. These errors mainly occur in the areas along the Solitario Canyon, Iron Ridge, and Highway-95 faults where the hydraulic gradient is quite steep. In these two steep gradient areas, most of the residual errors are because of limitations of the model grid and are not problematic. For example, consider that approximately a 50-m [164 ft] drop in head occurs across the Solitario Canyon fault. By limiting the width of the fault to a single row of grid cells, the head drop in the numerical model must occur over the 300-m [984 ft] width of a grid cell, whereas the water level analysis depicted in Figure 2-2 shows the same head drop over a distance of more than 1 km [0.62 mi]. Thus, much of the residual calibration error could be reduced in the model by adjusting the widths or positions of the Solitario Canyon-Iron Ridge and Highway-95 fault zones.

Hydraulically down gradient from Yucca Mountain, where observed heads are between 730 and 715 m [2,394 ft and 2,345 ft], model calibration is generally good. Most residual errors are less than 10 m [33 ft] and evenly distributed above and below zero. Some of the highest residual errors in this area are for an observation point near the Highway-95 fault. Other significant residual errors are present along potential flow paths from Yucca Mountain beneath the Fortymile Wash area where observed heads are between 720 and 725 m [2,362 ft and 2,378 ft]. This error can be seen

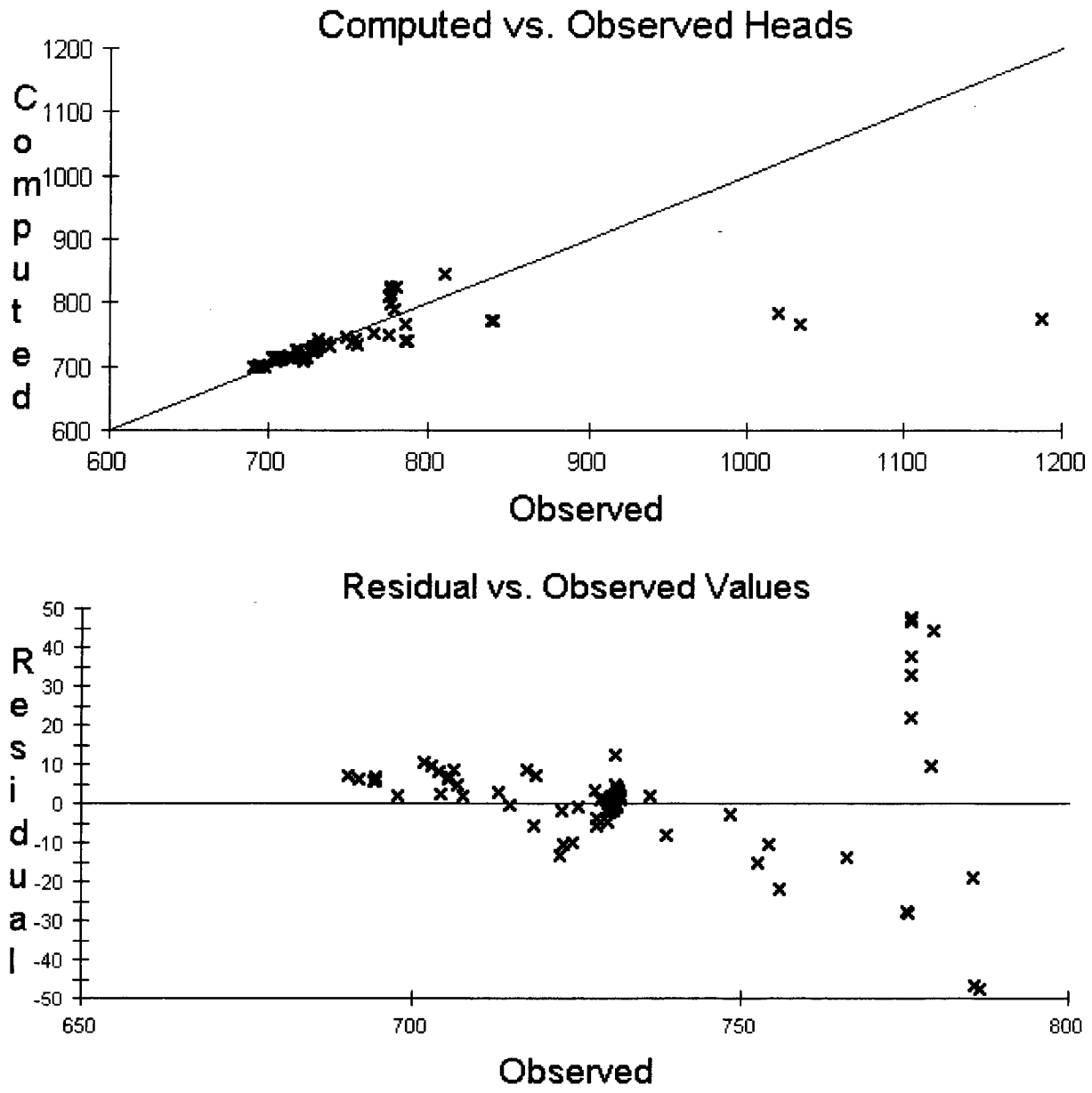

Figure 3-4. Plots Showing Relationships Between Observed Hydraulic Heads and Calculated Heads (Upper) and Residual Model Error (Lower) for the Approach 1 Calibrated Model

by comparing the calibrated head contours in Figure 3-1 to the water table contours in Figure 2-2: the 720 and 725-m [2,362-ft and 2,378-ft] head contours predicted by the model in Figure 3-1 are too far north by several kilometers.

In the southernmost portion of the model where observed heads are below 715 m [2,345 ft], residual errors are biased to the positive side of zero. Possible explanations for this bias are that it may be caused by error in the interpreted water table elevations used to define the

constant-head boundary in this area or by the assumption that the hydraulic conductivity of alluvium is homogenous.

The calibrated hydraulic conductivity values for each layer and structural feature are listed in Table 3-1. Most of the calibrated hydraulic conductivity values are within the ranges of initial estimates discussed in Section 2.5, except for the Upper Volcanic Confining layer and the Paleozoic Aquifer. The value of 10^{-3} m/d [0.025 gal/d/ft^2] for the Upper Volcanic Confining layer is an order of magnitude below the initially estimated range (Section 2.5.1), but is generally consistent with the conceptualization of the Upper Volcanic Confining layer as semiconfining.

The value of 10^{-4} m/d [0.0025 gal/d/ft^2] for the Paleozoic Aquifer is three orders of magnitude lower than the estimate at Well p#1 and is not consistent with the conceptualization that the Paleozoic Aquifer represents a relatively permeable aquifer formation. Still, considerable uncertainty exists in the appropriate hydraulic conductivity for the Paleozoic Aquifer, and such a low value cannot be ruled out. On examination of the model results, however, it seemed evident that a reasonable calibration could be obtained with a higher hydraulic conductivity value for the Paleozoic Aquifer, if one could assume that the portion of the Paleozoic Aquifer in the northeast portion of the model had a reduced hydraulic conductivity near the caldera complex.

A model approach that explicitly considers alteration of material properties within the caldera zone is presented in the following section.

3.2 Model Calibration Approach 2: Including Caldera Complex

The second approach is nearly identical to first approach, except that the northern boundary condition is set to a constant head of 1,100 m [3,608 ft], and two new material types are included for consideration of hydrologic properties altered by the caldera complex. The two new materials represent caldera-altered volcanic and Paleozoic rocks and are discussed in Section 2.5.3.

Hydraulic heads calculated for grid layer 7 of the calibrated Approach 2 model are illustrated in the contour map in Figure 3-5. Similar to Approach 1, calculated heads in the area of interest for flow paths from Yucca Mountain compare favorably to the water table elevation map in Figure 2-2. Effects of structure and layering on the distribution of hydraulic heads, illustrated in Figure 3-6, are also similar to Approach 1 results.

Much improved in this model is the match to the observed upward hydraulic gradient across the Lower Volcanic Confining layer, shown in Figure 3-7. The calculated head for the p#1 monitored (red square) interval is 753.2 m [2,470.5 ft], which compares well to the observed head of 752.9 m [2,469.5 ft] (Graves, 2000). Additionally, the 23-m [75-ft] calculated head difference across the Lower Volcanic Confining layer closely matches the observed 23-m [75-ft] head drop in Well p#1. By introducing a zone of low-permeability Paleozoic rock (Caldera_PZ) in the caldera complex, the remainder of the Paleozoic Aquifer can be assigned a higher hydraulic conductivity that allows higher heads from the north end of the model to propagate farther southward in the Paleozoic Aquifer. The geometry of the Caldera_PZ zone can be seen in Figures 3-6 and 3-7.

Table 3-1. Calibrated Hydraulic Conductivity Values for Approach 1 with No Caldera Complex and a No-Flow Northern Boundary Condition	
Model Layer/Feature	**Calibrated Hydraulic Conductivity**
Alluvium	10.0 m/d [250 gal/d/ft^2]
Upper Volcanic Aquifer (UVA)	10.0 m/d [250 gal/d/ft^2]
Upper Volcanic Confining Layer (UVC)	10^{-3} m/d [00.25 gal/d/ft^2]
Lower Volcanic Aquifer (LVA)	0.1 m/d [2.5 gal/d/ft^2]
Lower Volcanic Confining Layer (LVC)	10^{-5} m/d [2.5×10^{-4} gal/d/ft^2]
Paleozoic Aquifer (PZ)	10^{-4} m/d [2.5×10^{-3} gal/d/ft^2]
Bow Ridge–Paintbrush Canyon Fault Zone (BR-PBC_Flt)	1.0 m/d [25 gal/d/ft^2]
Solitario Canyon–Iron Ridge Fault System (SC-IR_Flt)	10^{-4} m/d [2.5×10^{-3} gal/d/ft^2]
Solitario Canyon Western Splay Fault (SC-west_Flt)	10^{-3} m/d [0.025 gal/d/ft^2]
Highway-95 Fault (H95)	10^{-3} m/d [0.025 gal/d/ft^2]
Fortymile Wash Fault (FMW_Flt)	10.0 m/d [250 gal/d/ft^2]
Bare Mountain Fault (BM_Flt)	10^{-3} m/d [0.025 gal/d/ft^2]
Crater Flat Fault (CF_Flt)	10^{-3} m/d [0.025 gal/d/ft^2]
VH–1 Fault (VH1_Flt)	10^{-3} m/d [0.025 gal/d/ft^2]
Central Amargosa Fault (CA_Flt)	1.0 m/d [25 gal/d/ft^2]
Gravity Fault #1 (Grav1_Flt)	1.0 m/d [25 gal/d/ft^2]
Gravity Fault #2 (Grav2_Flt)	1.0 m/d [25 gal/d/ft^2]

The plots in Figure 3-8 show comparisons of observed hydraulic heads to calculated heads (upper plot) and to residual calibration error (lower plot) for the Approach 2 model. It can be seen by comparing Figure 3-8 to Figure 3-4 that the overall quality of the Approach 2 model calibration is qualitatively similar to Approach 1. While the introduction of the Caldera_Paleozoic Aquifer zone improved the calibration to the deep observation point at Well p#1, the caldera-altered volcanic rock (Caldera_VR) does not appear to affect significantly the model calibration. A notable exception is that theApproach 2 model provides a better match to the highest observed head value of 1,187 m [3,893 ft], which is near the northern boundary of the model. It is not clear that the lower residual error calculated for this observation point represents an improved calibration, however, because the high observed head near the north boundary may represent perched water. Possible explanations for differences between observed and modeled heads in other areas of the Approach 2 model are identical to those given for Approach 1 and are not repeated here.

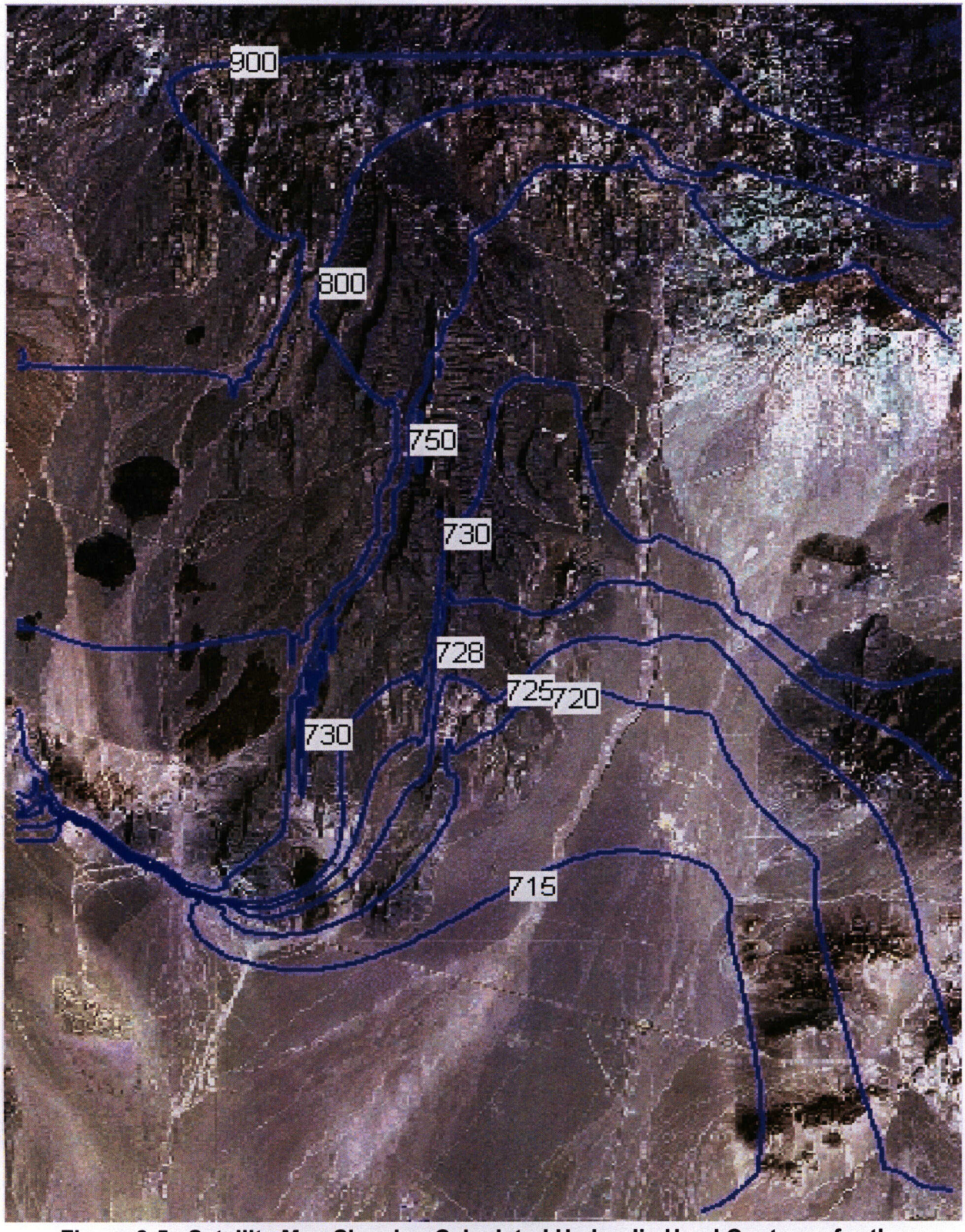

Figure 3-5. Satellite Map Showing Calculated Hydraulic Head Contours for the Approach 2 Flow Model Calibration

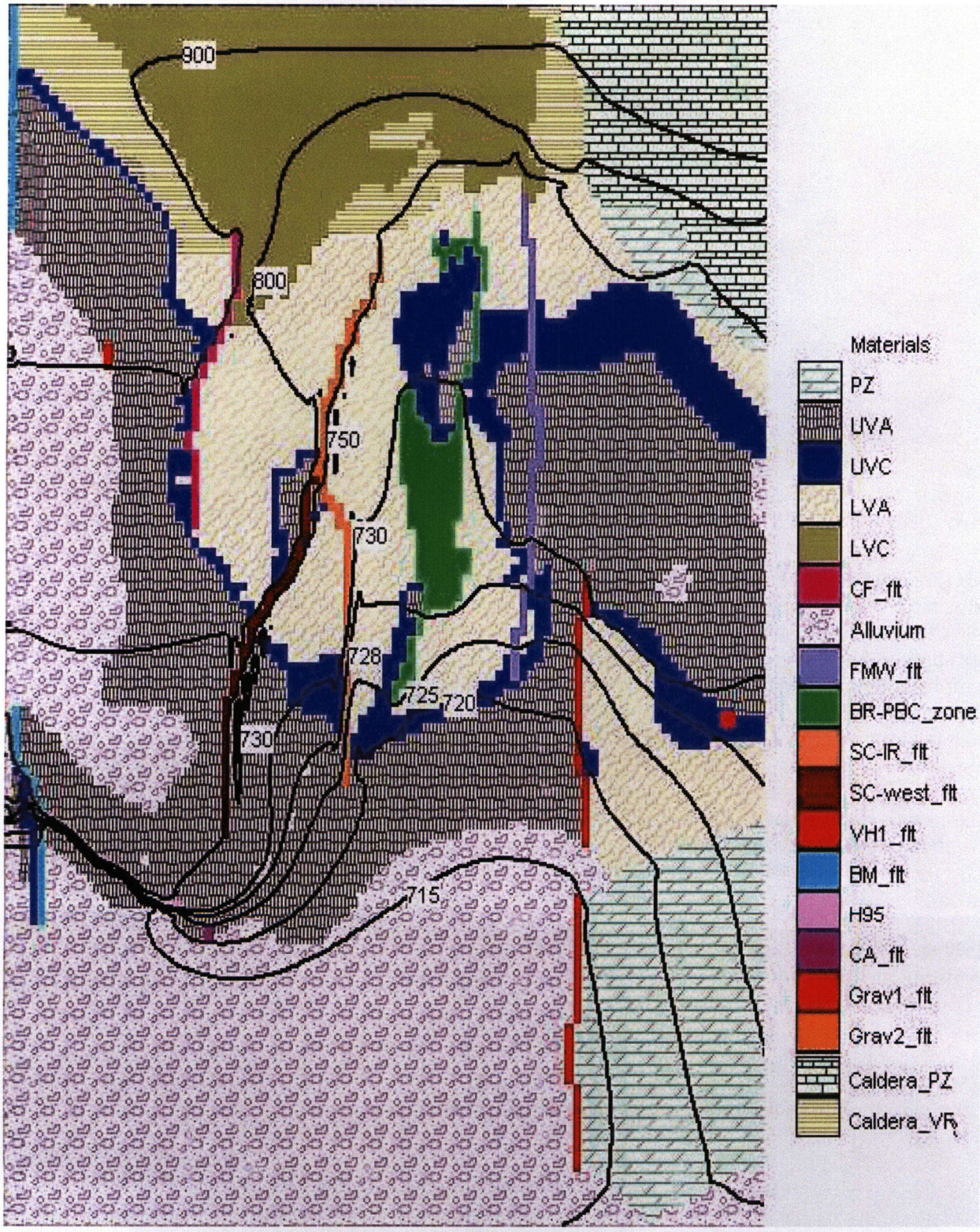

Figure 3-6. Map Showing Constant-Head Contour Lines Calculated for the Approach 2 Flow Model Calibration in Relation to Hydrostratigraphic and Structural Features (see Table 3-2 for material designations in legend)

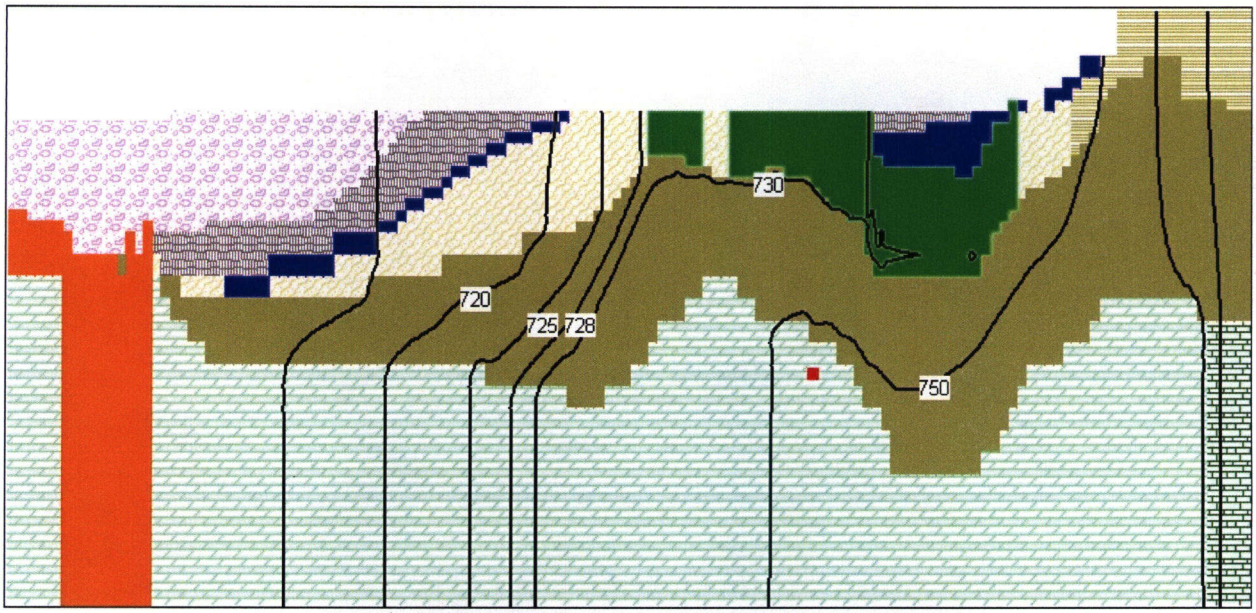

Figure 3-7. North-South Cross Section of Calibrated Approach 2 Flow Model Passes Through Well UE–25 p#1 Monitored Interval (Red Square) Just West of Fortymile Wash

Calibrated hydraulic conductivity values for each layer and structural feature of the Approach 2 model are listed in Table 3-2. In Approach 2, all calibrated hydraulic conductivity values are within the ranges of initial estimates discussed in Section 2.5. Thus, although the overall calibration of Approach 2 is not significantly improved from Approach 1, the calibrated values are more consistent with the conceptualization of hydrologic properties given in Section 2.5. For example, it was possible to increase the assigned hydraulic conductivity of the Upper Volcanic Confining layer from 10^{-3} m/d [0.025 gal/d/ft^2] to 0.05 m/d [1.25 gal/d/ft^2], which is more consistent with the 0.01–0.1 m/d [0.25–2.5 gal/d/ft^2] range estimated for the Upper Volcanic Confining Layer in Section 2.5.1. Hydraulic conductivities of Alluvium and the Upper Volcanic Aquifer were decreased to 7.0 m/d [175 gal/d/ft^2] and 5.0 m/d [125 gal/d/ft^2] in the Approach 2 calibration. This is closer to the middle of the range estimated for these parameters in Section 2.5.1, compared to the value of 10 m/d [250 gal/d/ft^2] for both these parameters in Approach 1, which is at the limit of the estimated range.

Hydraulic conductivity assigned to the Solitario Canyon and Iron Ridge faults for Approach 2 was increased from 10^{-4} to 10^{-3} m/d [2.5×10^{-3} to 0.025 gal/d/ft^2] compared to Approach 1. Interestingly, this order-of-magnitude change in the Solitario Canyon and Iron Ridge faults properties did not have much effect on the model calibration. It can be presumed, however, that continuing to increase the hydraulic conductivity of the Solitario Canyon-Iron Ridge fault system would at some point have a marked effect on model calibration, given its importance to reproducing the steep hydraulic gradient associated with this feature.

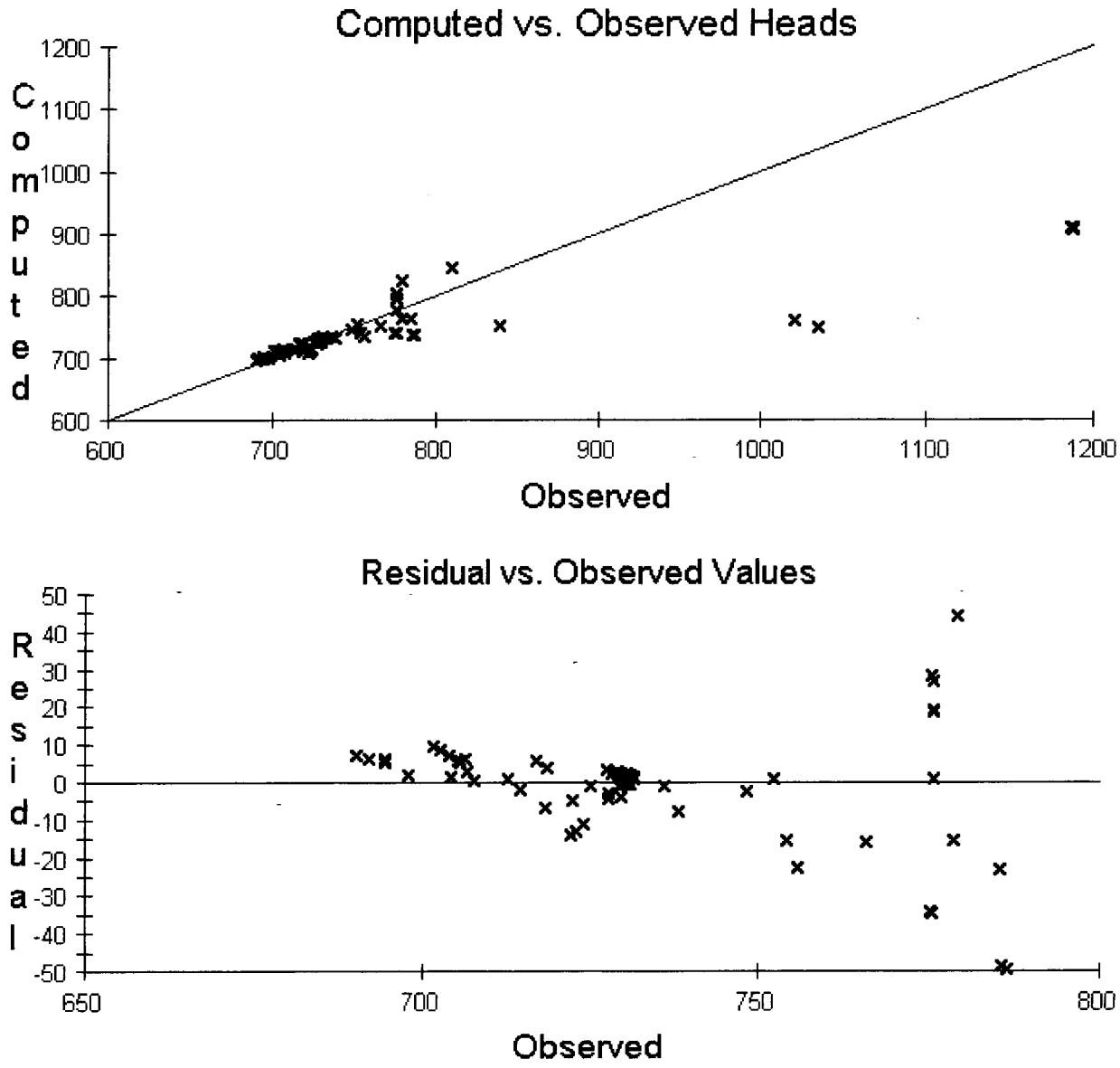

Figure 3-8. Plots Showing Relationships Between Observed Hydraulic Heads and Calculated Heads (Upper) and Residual Model Error (Lower) for the Approach 2 Calibrated Model

Table 3-2. Calibrated Hydraulic Conductivity Values for Approach 2 with Caldera Complex Defined in the Northern Model Region	
Model Layer/Feature	**Calibrated Hydraulic Conductivity**
Alluvium	7.0 m/d [175 gal/d/ft^2]
Upper Volcanic Aquifer (UVA)	5.0 m/d [125 gal/d/ft^2]
Upper Volcanic Confining Layer (UVC)	0.05 m/d [1.25 gal/d/ft^2]
Lower Volcanic Aquifer (LVA)	0.1 m/d [2.5 gal/d/ft^2]
Lower Volcanic Confining Layer (LVC)	10^{-5} m/d [2.5×10^{-4} gal/d/ft^2]
Paleozoic Aquifer (PZ)	0.1 m/d [2.5 gal/d/ft^2]
Bow Ridge–Paintbrush Canyon Fault Zone (BR-PBC_Flt)	10.0 m/d [250 gal/d/ft^2]
Solitario Canyon–Iron Ridge Fault System (SC-IR_Flt)	10^{-3} m/d [0.025 gal/d/ft^2]
Solitario Canyon Western Splay Fault (SC-west_Flt)	10^{-3} m/d [0.025 gal/d/ft^2]
Highway-95 Fault (H-95)	10^{-3} m/d [0.025 gal/d/ft^2]
Fortymile Wash Fault (FMW_Flt)	10.0 m/d [250 gal/d/ft^2]
Bare Mountain Fault (BM_Flt)	10^{-3} m/d [0.025 gal/d/ft^2]
Crater Flat Fault (CF-Flt)	10^{-3} m/d [0.025 gal/d/ft^2]
VH–1 Fault (VH1_Flt)	10^{-3} m/d [0.025 gal/d/ft^2]
Central Amargosa Fault (CA_Flt)	1.0 m/d [25 gal/d/ft^2]
Gravity Fault #1 (Grav1_Flt)	0.1 m/d [2.5 gal/d/ft^2]
Gravity Fault #2 (Grav2_Flt)	1.0 m/d [25 gal/d/ft^2]
Caldera-Altered Paleozoic Rock (Caldera-PZ)	10^{-3} m/d [0.025 gal/d/ft^2]
Caldera-Altered Volcanic Rock (Caldera-VR)	10^{-5} m/d [2.5×10^{-4} gal/d/ft^2]

4 DISCUSSION, CONCLUSIONS, AND RECOMMENDATIONS

Development of an independent site-scale flow model for the Yucca Mountain region provides useful insights for reviewing the DOE model. Problems encountered during the development process can be compared with the DOE approach to evaluate whether its model is subject to similar problems.

4.1 Comparison of Results to the U.S. Department of Energy Model

There are several differences between the CNWRA and the DOE saturated zone flow models. For example, the Hydrogeologic Framework Model used as the foundation for the CNWRA model has only 6 hydrostratigraphic layer types, compared to the 18 layer types used in the DOE model (CRWMS M&O, 2000). Additionally, treatment of the low-permeability zone to the north is different for the two models: the DOE model defines four different zones of altered permeability in the northern area, whereas the CNWRA model uses only two altered material types to represent this area.

The reduced hydrogeologic complexity notwithstanding, the calculated hydraulic head distribution from the CNWRA model calibration is qualitatively similar to the DOE calibrated flow model (CRWMS M&O, 2000, Figure 7). Except for the northernmost area of the model, residual errors between observed and calibrated head values are generally less than 50 m [164 ft] in both models. Residual errors in both models are between 0 and 5 m [16.4 ft] in the area of interest between Yucca Mountain and the 18-km [11.2-mi] compliance boundary.

In the northern model area, the DOE model does a better job to match water levels observed in wells. An explanation for this difference is that, in the CNWRA model, the observed high water levels in this area are conceptualized as perched water, and the northern boundary condition was set to a level nearly 100 m [328 ft] lower than what is observed in the northernmost observation well. Note that, in documentation of the DOE Flow Model (CRWMS M&O, 2000), three wells in the northern model area are suspected of being completed in perched water bodies.

4.2 Recommendations

This report documents development of the CNWRA three-dimensional, site-scale saturated zone flow model. Although this process is insightful for reviewing the DOE performance assessment abstraction for saturated zone flow, none of the analyses in this report have been specifically directed at evaluating the DOE approach. Now that the model has been developed and reasonably calibrated, it can be used as a tool to evaluate the potential effects of various data and model uncertainties on saturated zone flow paths. Those evaluations can then be used for comparison with the level of uncertainty considered in the DOE performance assessments resulting from factors such as groundwater specific discharge (flux) and flow path lengths through various material types. Additionally, evaluation of data and model uncertainties can be used to improve the saturated zone flow abstraction in the NRC independent performance assessment code. The following recommendations are made for future analyses using the CNWRA model to evaluate data and model uncertainty.

- Inverse optimization methods should be employed to refine the model calibration from the current trial-and-error calibration and to obtain a ranking of parameter sensitivities. Inverse optimization can also be employed to recalibrate the model when alternative scenarios, such as modified boundary conditions, are evaluated.

- Effects of water table recharge associated with higher elevation areas and the Fortymile Wash area should be evaluated.

- Boundary condition uncertainties should be evaluated. These uncertainties include the assumption of constant head with depth, uncertainty in the distribution of head values interpreted from water table maps, and uncertainty in the appropriate head values for the northern boundary.

- Possible effects of vertical and horizontal anisotropies in hydraulic conductivity should be evaluated.

- Effects of changing the geometry of the Bow Ridge–Paintbrush Canyon fault zone should be examined. For example, this zone may extend as far east as the Fortymile Wash fault.

- More detailed analyses of potential effects of fault zones on flow should be conducted. For the analyses in this report, many of the faults were assigned an arbitrary hydraulic conductivity.

4.3 Conclusion

This report documents development of a three-dimensional, site-scale groundwater flow model for the saturated zone beneath Yucca Mountain, Nevada. Initial attempts at model calibration demonstrated that consideration of geologic structure and some type of barrier to lateral flow in the northern portion of the model are necessary. After inclusion of the geologic structure, a reasonable calibration was obtained that is generally consistent with observed water levels in the area of interest down gradient from Yucca Mountain. When altered properties associated with the caldera zone are also included in the northern portion of the model, the model provides improved agreement with the observed upward vertical gradient across the Lower Volcanic Confining Layer. The residual error in this model calibration is of similar magnitude to that of the DOE saturated flow model. Future work will include use of inverse optimization methods to obtain calibrations for various approach analyses to quantify the effects of data and model uncertainties on saturated zone flow paths. Such analyses are necessary to support development of the NRC independent performance assessment code and to develop a knowledge base for risk-informed NRC review of the DOE performance assessments for Yucca Mountain.

5 REFERENCES

Craig, R.W. and J.H. Robison. "Geohydrology of Rocks Penetrated by Test Well UE–25p#1." U.S. Geological Survey Water Resources Investigations Report 84-4248. 1984.

CRWMS M&O. "Calibration of the Site-Scale Saturated Zone Flow Model." MDL–NBS–HS–000011. Revision 00. Las Vegas, Nevada: CRWMS M&O. 2000.

Environmental Modeling Research Laboratory. "The Department of Defense Groundwater Modeling System, GMS v3.0 Reference Manual." Salt Lake City, Utah: Brigham Young University, Environmental Modeling Research Laboratory. 1999.

Geldon, A.L. "Preliminary Hydrogeologic Assessment of Boreholes UE–25c#1, UE–25c#2, and UE–25c#3, Yucca Mountain, Nye County, Nevada." U.S. Geological Survey Water Resources Investigations Report 92-4016. 1993.

Geldon, A.L., A.M.A. Umari, J.D. Earle, M.F. Fahy, J.M. Gemmel, and J. Darnell. "Analysis of a Multiple-Well Interference Test in Miocene Tuffaceous Rocks at the C-Holes Complex, May–June, 1995, Yucca Mountain, Nye County, Nevada." U.S. Geological Survey Water Resources Investigations Report 94-4166. 1998.

Graves, R.P. "Water Levels in the Yucca Mountain Area, Nevada, 1997–1998." U.S. Geological Survey Open-File Report 00-186. 2000.

Harbaugh, A.W. and M.G. McDonald. "User's Documentation for MODFLOW-96, An Update to the U.S. Geological Survey Modular Finite-Difference Ground Water Flow Model." U.S. Geological Survey Open File Report 96-485. 1996.

LeCain, G.D. "Results from Air-Injection and Tracer Testing in the Upper Tiva Canyon, Bow Ridge Fault, and Upper Paintbrush Contact Alcoves of the Exploratory Studies Facility, August 1994 through July 1996, Yucca Mountain, Nevada." U.S. Geological Survey Water Resources Investigations Report 98-4058. 1998.

LeCain, G.D., L.O. Anna, and M.F. Fahy. "Results from Geothermal Logging, Air and Core-Water Chemistry Sampling, Air-Injection Testing and Tracer Testing in the Northern Ghost Dance Fault, Yucca Mountain, Nevada, November 1996 to August 1998." U.S. Geological Survey Water Resources Investigations Report 99-4210. 1999.

Luckey, R.R., P. Tucci, C.C. Faunt, E.M. Ervin, W.C. Steinkampf, F.A. D'Agnese, and G.L. Patterson. "Status of Understanding of the Saturated-Zone Ground-Water Flow System at Yucca Mountain, Nevada, as of 1995." U.S. Geological Survey Water-Resources Investigations Report 96-4077. 1996.

Painter, S., J.R. Winterle, and A. Armstrong. "Alternative Explanation for Groundwater Temperature Variations Near Yucca Mountain, Nevada." San Antonio, Texas: CNWRA. 2002.

Plume, R.W. and R.J. La Camera. "Hydrogeology of Rocks Penetrated by Test Well JF–3, Jackass Flats, Nye County, Nevada." U.S. Geological Survey Water Resources Investigations Report 95-4245. 1996.

Sims, D.W., J.A. Stamatakos, D.A. Ferrill, H.L. McKague, D.A. Farrell, and A. Armstrong. "Three-Dimensional Structural Model of the Amargosa Desert, Version 1.0: Report to Accompany Model Transfer to the Nuclear Regulatory Commission." San Antonio, Texas: CNWRA. 1999.

Thordarson, W. "Geohydrologic Data and Test Results from Well J–13, Nevada Test Site, Nye County, Nevada." U.S. Geological Survey Water-Resources Investigations Report 83-4171. 1983.

Winterle, J.R. and P.C. La Femina. "Review and Analyses of Hydraulic and Tracer Testing at the C-Holes Complex Near Yucca Mountain, Nevada." San Antonio, Texas: CNWRA. 1999.

Winterle, J.R., N.M. Coleman, W.A. Illman, and D. Hughson. "Review of Permeability Estimates Obtained from the Yucca Mountain Project." San Antonio, Texas: CNWRA. 2000.